CHEMISTRY
A EUROPEAN JOURNAL

DOI: 10.1002/chem.200700819

Non-Cytotoxic, Bifunctional Eu^{III} and Tb^{III} Luminescent Macrocyclic Complexes for Luminescence Resonant Energy-Transfer Experiments

Anne-Claire Ferrand,[a] Daniel Imbert,[a, b] Anne-Sophie Chauvin,[a] Caroline D. B. Vandevyver,[a] and Jean-Claude G. Bünzli*[a]

Abstract: A new macrocyclic ligand, L^3, has been synthesised, based on the cyclen framework grafted with three phenacyl light-harvesting groups and a C_5-alkyl chain bearing a carboxylic acid function as a potential linker for biological material. Acidity constants are determined by spectrophotometric titrations, as well as conditional stability constants for the resulting 1:1 complexes with trivalent lanthanide ions. The complexes have stabilities comparable to 1,4,7,10-tetrakis(carbamoylmethyl)-1,4,7,10-tetraazacyclododecane (dtma) complexes, with $pLn \approx 12$–13. Photophysical properties of the ligand and of the EuL^3 and TbL^3 complexes have been determined for both microcrystalline samples and solutions in water and acetonitrile. They point to the metal ion being present in an environment with axial symmetry derived from the C_4 point group. The hydration number determined for TbL^3 decreases with increasing pH value and becomes fractional at pH 7.5, which points to an equilibrium between two differently solvated species and probably to the participation of the deprotonated carboxylic acid chain in the complexation. The quantum yields in water (1.9% for Eu^{III}, 3.4% for Tb^{III}) are smaller than those for complexes with the symmetrically substituted parent macrocycle, but efficient luminescence resonant energy transfer (LRET) was observed when Cy5 dye was added to the solutions. Finally, the influence of the TbL^3 complex on cell viability is tested on both malignant (5D10 mouse hybridoma, Jurkat human T leukaemia, MCF-7 human breast carcinoma) and non-malignant (Hacat human keratinocyte) cell lines. Cell viability after 24 h incubation at 37 °C with 500 μM TbL^3 was >90% for all cell lines, except Jurkat (>70%). All of these properties make LnL^3 complexes interesting potential probes for bioanalyses.

Keywords: cytotoxicity · energy transfer · lanthanides · luminescence · macrocyclic ligands

Introduction

The synthesis of the tetracarboxylic acid derivative of cyclen (1,4,7,10-tetraazacyclododecane), H_4dota, and of some of its d-transition-metal complexes by Stetter and Frank in 1976[1] was followed three years later by the recognition that this derivatised macrocycle is ideally suited for the complexation of trivalent lanthanides (Ln^{III}) in water.[2] The resulting ennea-coordinate complexes are thermodynamically stable and kinetically inert and they feature one water molecule occupying the axial site.[3] These properties, together with large LD_{50} values,[4] stirred immediate interest for bioinorganic and medical applications, the first of which was in the design of contrast agents for magnetic resonance imaging, for example $[Gd(dota)(H_2O)]^-$,[5] a field that has generated a wealth of developments during the last 20 years.[6] The distinctive photophysical properties of Ln^{III} ions,[7] which emit line-like, easily recognisable luminescence spectra and have long excited-state lifetimes, open the way to highly sensitive time-resolved bioanalyses.[8,9] These properties can be adequately tuned in complexes with cyclen derivatives, in particular by grafting sensitising and/or coordinating groups onto the macrocycle scaffold for light harvesting and subsequent energy transfer onto the metal ion. Laporte forbidden f–f transitions are too weak to be efficient vectors for Ln^{III} excitation and the cyclen framework in itself is not a good

[a] Dr. A.-C. Ferrand, Dr. D. Imbert, Dr. A.-S. Chauvin, Dr. C. D. B. Vandevyver, Prof. Dr. J.-C. G. Bünzli
École Polytechnique Fédérale de Lausanne
Laboratory of Lanthanide Supramolecular Chemistry
BCH 1402, 1015 Lausanne (Switzerland)
Fax: (+41) 21-698-9825
E-mail: jean-claude.bunzli@epfl.ch

[b] Dr. D. Imbert
Laboratoire de Reconnaissance Ionique
UMR-E3 CEA-UJF, DRFMC
CEA-Grenoble (France)

Supporting information for this article is available on the WWW under http://www.chemeurj.org/ or from the author.

chromophore. The first sensitising group tested was carbostyril 124 (7-amino-4-methyl-2-(1*H*)-quinolinone),[10] with modest results as far as the tetraamide derivative of cyclen, 1,4,7,10-tetrakis(carbamoylmethyl)-1,4,7,10-tetraazacyclododecane (dtma), is concerned.[11] Other sensitising groups were rapidly proposed[12] and rich chemistry and analytical applications were developed, for instance, for sensing pH, pO_2 and biorelevant anion values[13–16] or for producing highly luminescent thin films for light-emitting diodes.[17] Lanthanide-containing responsive luminescent probes tailored from cyclen derivatives are presently ubiquitous tools in bioanalyses. Lately, they have sustained further engineering so that in cellulo molecular imaging and sensing have become feasible, by making use of both visible and near-infrared metal-based luminescence.[18,19]

In our laboratories, we pursue the development of visible[20] and near-infrared[21] luminescent probes through several strategies, one of which is based on dtma derivatives (Scheme 1).[22,23] In particular, we have shown that ligands L^1 and L^2 react with lanthanide triflates to form stable 1:1 complexes in water, as shown by the pLn values[24] for L^1 (7.5 and 9 for Eu^{III} and Tb^{III}) and by the fact that log*K* $\approx$12–13 for L^2. The metal-centred luminescence of the Sm^{III}, Eu^{III}, Tb^{III} and Dy^{III} complexes is sensitised to a variable extent; the best chromophore for Eu^{III} is the phenylphenacyl group, while the phenacyl group is best suited for energy transfer on Tb^{III}.[25] Building on the latter work, we have now replaced one phenacyl substituent with an aliphatic chain bearing a carboxylic acid function; this group, along with primary amine, chlorosulfonyl and isothiocyanate, is among the most common linking moieties that can covalently interact with biologically relevant molecules such as proteins.[26] The aim of this study is to examine the influence of this substitution on both the thermodynamic and photophysical properties of the resulting lanthanide complexes. In addition, we establish that LnL^3 (Ln: Eu, Tb) complexes efficiently transfer energy on cyanine 5 (Cy5), a dye used in luminescence resonance energy transfer (LRET) experiments (for example, in evidencing DNA hybridisation)[27] and in homogeneous luminescence immunoassays.[28] Finally, the influence of the TbL^3 complex on cell viability is tested on various malignant and non-malignant cell lines.

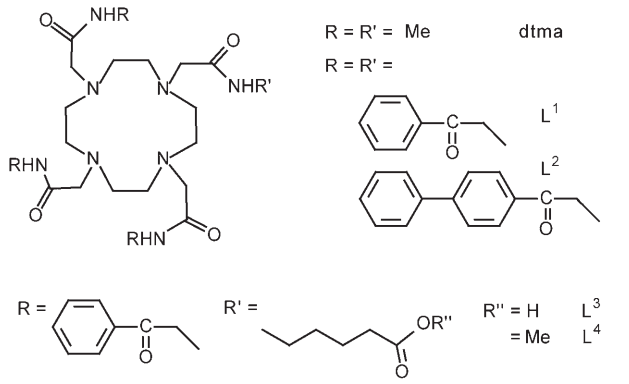

Scheme 1. Ligand formulae

Results and Discussion

Ligand synthesis and acid–base properties: Ligand synthesis followed the now-classical regioselective method proposed for introducing 3+1 substituents on the cyclen scaffold.[29,30] The carboxylic acid substituent **1** was obtained from bromoacetyl bromide and 6-aminocaproic acid (Scheme 2), while the phenacyl pendant **3** was synthesised as previously described.[25] One amine function of cyclen was protected by the method of Platzek et al. for 1,7-substituted cyclens:[31] *N*,*N*-dimethylformamide dimethylacetal (DMF-DMA) was treated with cyclen to produce 1,4,7,10-tetraazatricyclo-

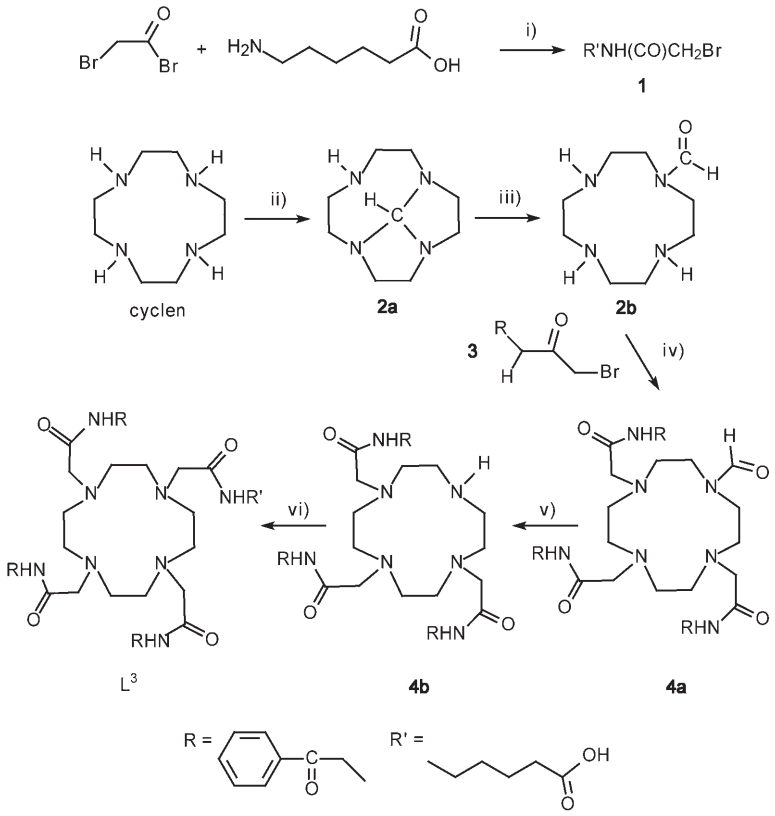

Scheme 2. i) 4 M NaOH, H_2O, 0 °C; ii) *N*,*N*-dimethylformamide dimethylacetal, toluene, 120 °C; iii) EtOH, H_2O, −18 °C; iv) **3**, NEt_3, THF; v) HCl_{aq}, H_2O/acetone; vi) **1**, Cs_2CO_3, MeCN, 24 h, RT.

[5.5.1.0]tridecane (**2a**) in almost quantitative yield and upon careful hydrolysis at low temperature this produced the formaldehyde-protected material **2b**. Use of a quasistoichiometric quantity of DMF-DMA (1.05 equivalents) resulted in avoidance of the formation of the diformylated product. A classical reaction between the three unprotected amine functions of **2b** and *N*-(phenacyl)bromoacetamide (**3**) in the presence of triethylamine afforded **4a** in 65% yield. The final substitution reaction leading to L^3 has been optimised with respect to the choice of solvent (chloroform, THF, MeCN) and base (no base, triethylamine, Hüning base, potassium and caesium carbonates), as well as the reaction time. The best experimental conditions turned out to be with one equivalent of caesium carbonate in acetonitrile: a 24 h reaction time at room temperature afforded L^3 in 30% yield, while most of the starting macrocycle **4b** could be recycled and no secondary product was formed. Such products form as soon as the reaction time is increased, while the absence of base or the presence of a different base leads to smaller conversion rates. Ligand L^4 was synthesised with the purpose of confirming the pK_a assignment for L^3; it was obtained in 43% yield by refluxing L^3 overnight in methanol.

Potentiometric titration of a 1.02 mM aqueous solution of L^3 adjusted to pH 1.5 with hydrochloric acid, was performed with NaOH 0.1 M up to pH 12.5. Data could be satisfyingly fitted to the following set of equations and protonation constants:

$$(L^3)^-_{aq} + H^+ \rightleftharpoons (HL^3)_{aq} \qquad \log K_{a1} = 11.42 \qquad (1)$$

$$(HL^3)_{aq} + H^+ \rightleftharpoons (H_2L^3)^+_{aq} \qquad \log K_{a2} = 9.51 \qquad (2)$$

$$(H_2L^3)^+_{aq} + H^+ \rightleftharpoons (H_3L^3)^{2+}_{aq} \qquad \log K_{a3} = 5.65 \qquad (3)$$

$$(H_3L^3)^{2+}_{aq} + H^+ \rightleftharpoons (H_4L^3)^{3+}_{aq} \qquad \log K_{aCarb} = 4.49 \qquad (4)$$

$$(H_4L^3)^{3+}_{aq} + H^+ \rightleftharpoons (H_5L^3)^{4+}_{aq} \qquad \log K_{a5} = 1.97 \qquad (5)$$

Assignment of pK_{aCarb} to the carboxylic acid function of the pendant arm is straightforward when the $\log K_a$s are compared to those obtained under the same experimental conditions for ligand L^4 and to literature values for dtma[32] (Table 1). Only four protonation constants could be determined for L^4. The first three have values close to the first three $\log K_a$ values of L^3, while the fourth is close to the $\log K_{a5}$ value for L^3. The value of around 4.5 for L^3 is missing for L^4, so it can confidently be assigned as arising from the carboxylic acid function ($\log K_{aCarb}$). The large value of the latter may arise from stabilisation through hydrogen bonding, much as carboxylate groups can assist protonation of ligand amine groups.[32] This would imply that the carboxylic acid arm folds over the macrocycle, a hypothesis that may be substantiated by the hydration numbers determined for TbL^3 (see below). Another conclusion is that the replacement of one amide pendant by the C_5 carboxylic acid chain does not noticeably influence the protonation constants of the macrocycle amine functions. A comparison of the protonation constants found for L^3 and L^4 with published data for dtma is more delicate since only three $\log K_a$ values are reported for this macrocycle.[32] The smallest protonation constant is comparable to the $\log K_{a4}$ value for L^4 and the middle value is a reasonable match with the $\log K_{a3}$ values for L^3 and L^4. On the other hand, the largest value corresponds to the $\log K_{a2}$ value of L^3 and L^4 and not the $\log K_{a1}$ value. A distribution diagram for L^3 is shown in Figure S1 in the Supporting Information.

Table 1. Protonation constants for L^3 and L^4 as determined by potentiometric titration and comparison with corresponding data for dtma. Standard deviations are given within parentheses.

Ligand	$\log K_{a1}$	$\log K_{a2}$	$\log K_{a3}$	$\log K_{a4}$ or $\log K_{aCarb}$	$\log K_{a5}$
L^3	11.42(1)	9.51(2)	5.65(2)	4.49(2)	1.97(4)
L^4	11.25(1)	9.44(2)	5.94(1)	1.59(2)	
dtma[a]	9.27(1)	5.55(2)	1.56(7)		

[a] Data taken from reference [32].

Isolation and characterisation of the complexes: Complexes with formulae $[Ln(OTf)_3(L^3)]\cdot n\,MeCN\cdot m\,H_2O$ (Ln: Eu, Tb, Gd, Lu; OTf: triflate; $n = 0.5$ or 0; $m = 6$–7; denoted LnL^3 below) were readily obtained by mixing equivalent quantities of the lanthanide salt and the ligand in acetonitrile. To assess the stability of the 1:1 complexes in water, solutions containing equivalent amounts of ligand and lanthanide perchlorate, with a pH value set between 1.92 and 12.24, were equilibrated until thermodynamic equilibrium was reached and then their pH value was controlled and their absorption spectra were measured. Factor analysis yielded five data vectors and the spectra were fitted to Equations (6)–(8), in which the first $\log K$ values are for Eu^{III} complexes and the second are for those with Tb^{III}.

$$[Ln(L^3)]^{2+} + OH^- \rightleftharpoons [Ln(L^3)(OH)]^+ \qquad \log(K) = 5.9(4)/6.1(3) \qquad (6)$$

$$Ln^{3+}_{aq} + (L^3)^- \rightleftharpoons [Ln(L^3)]^{2+} \qquad \log(K) = 17.0(3)/16.3(2) \qquad (7)$$

$$[Ln(L^3)]^{2+} + H^+ \rightleftharpoons [Ln(HL^3)]^{3+} \qquad \log(K) = 26.0(3)/24.1(2) \qquad (8)$$

Convergence was very good for Eu^{III} ($\sigma = 4.46 \times 10^{-3}$) but somewhat less reliable for Tb^{III} ($\sigma = 1.14 \times 10^{-2}$). From these data and the protonation constants of L^3, the following pLn values[24] could be calculated: pEu = 13.4 and pTb = 11.6. In view of the less good adjustment obtained for Tb^{III}, the last value has to be considered as an estimate only and it is difficult to comment on the difference with respect to pEu. One may, however, conclude that ligand L^3 leads to reasonable stability of the 1:1 complexes in solution. The pLn values are comparable to those for dtma (for example, pGd = 12.4 when calculated from the constants reported by Bianchi et al.[32]), but smaller than the corresponding data for diethylene-trinitrolopentaacetic acid (dtpa) (for example, pGd =

19.8). A distribution diagram for Eu^{III} taking the protonation constants of L^3 into account is shown in Figure 1.

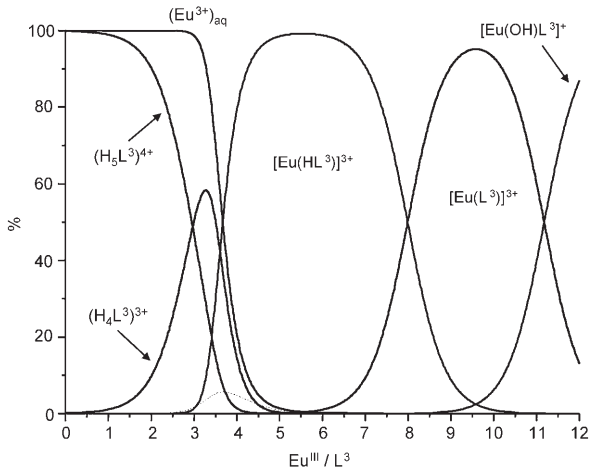

Figure 1. Distribution diagram for the system Eu^{III}/L^3 as calculated from spectrophotometric titrations in the pH range 1.92–12.24 at 25 °C and with $I = 0.1$ M (Me_4NCl).

Ligand-centred photophysical properties: The optical properties of ligand L^3 are similar to those reported previously for L^1.[25] The absorption maximum occurs at 247 nm (35 090 cm^{-1}, $\log\varepsilon = 4.58$) and no fluorescence is detected at 295 or 77 K in water/glycerol (95:5). Weak triplet-state emission is only seen at 77 K with a maximum at 420 nm (23 810 cm^{-1}) and a 0-phonon component at 390 nm (25 640 cm^{-1}); non observation of singlet-state fluorescence points to efficient non-radiative and/or intersystem crossing (isc) processes taking place in this molecule. The triplet-state energy is not much affected by the complexation; on the other hand, the phosphorescence spectra display a better intensity due to the heavy-atom effect of the lanthanide ion. All triplet-state emission spectra show vibrational components with an average spacing at around 1300–1400 cm^{-1}, which is typical of aromatic compounds. When recorded in fluorescence mode, the emission spectrum of LuL^3 features a very weak band on the high-energy side of the triplet-state emission peak ($\approx$370 nm, 27 000 cm^{-1}), which is tentatively assigned to singlet-state emission since this feature disappears upon enforcement of a time delay (Figure S2 in the Supporting Information). It is noteworthy that in addition to the narrow metal-centred emission, triplet phosphorescence is also seen for Eu^{III} and Tb^{III} complexes; in the latter case though, the metal-centred bands have a much larger integrated intensity than the ligand emission (Figure 2).

Metal-centred photophysical properties of microcrystalline complexes: Information on the metal-ion environment has been gained from high-resolution emission spectra of microcrystalline samples of the LnL^3 complexes (Ln: Eu, Tb) at 295 and 10 K. The room-temperature emission spectrum of

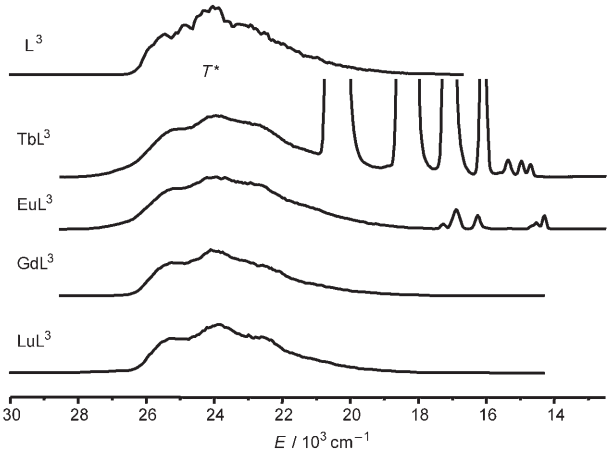

Figure 2. Phosphorescence spectra of L^3 and its lanthanide complexes in water/glycerol (95:5) at pH 6.5 and 77 K upon excitation at 40 320 cm^{-1} (248 nm). The spectra are not drawn to scale; the scale of the trace for the Tb complex has been expanded to show the triplet emission.

EuL^3 excited at 466 nm (21 460 cm^{-1}, $^5D_2$ level) is displayed in Figure 3. It is typical for a species (labelled I) with symmetry derived from a tetragonal arrangement.[25] The 0–0 transition appears as a mostly symmetrical band at

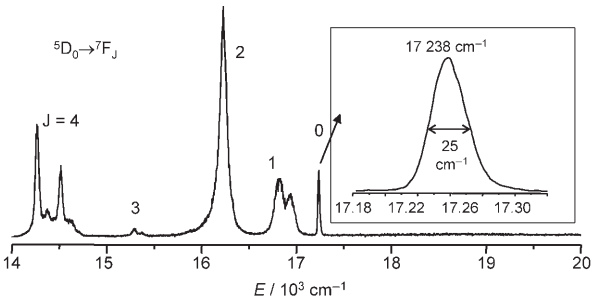

Figure 3. High-resolution emission spectrum of microcrystalline EuL^3 measured at 295 K upon $^5D_2 \rightarrow {}^7F_0$ excitation (21 460 cm^{-1}, 466 nm) and recorded in time-resolved mode. The inset shows an enlargement of the $^5D_0 \rightarrow {}^7F_0$ transition.

17 238 cm^{-1} (full width at half height (fwhh) = 25 cm^{-1}) and has sizeable oscillator strength with an intensity relative to the magnetic dipole transition $^5D_0 \rightarrow {}^7F_1$, I_0/I_1, equal to 0.15. It sustains the usual red shift (10 cm^{-1}) when the temperature is lowered to 10 K. Its room-temperature energy can, in principle, be estimated from the nephelauxetic effect generated by the coordinated donor groups[33] according to Equation (9), in which δ_i is the nephelauxetic effect of the donor group i and n_i is the number of coordinated donor groups.

$$\tilde{\nu}(\mathrm{cm^{-1}}, 295\ \mathrm{K}) = 17\,374 + \sum_i n_i\delta_i$$

With $\delta_i(\text{amide}) = -16.6$ cm and $\delta_i(\text{amine}) = -12.8$ cm^{-1},[33] we get a value of 17 256 cm^{-1} for an 8-coordinate Eu species. As the experimental value is 18 cm^{-1} smaller, the ninth coor-

dination position is most probably occupied. The Eu($^5D_0$) lifetime amounts to 0.94 ± 0.02 ms at 295 K, whatever the excitation mode is, through ligand or Eu^{III} levels, so that occupancy by water can be ruled out; a plausible alternative is coordination by the carboxylate group of the C_5 pendant arm. As a comparison, the Eu($^5D_0$) lifetime in EuL^1 is smaller, 0.60 ms, in line with the coordination of a water molecule, as demonstrated by X-ray crystallography for TbL^1.[25] Recalculation of $\tilde{\nu}$(0–0) with the nephelauxetic parameters above, scaled down for 9-coordination (−6%), and with δ_i(carboxy) = −17.2 cm^{-1}[33] yields a value of 17245 cm^{-1}, which is in fair agreement with the observed value.

A high-resolution scan of the 0–0 excitation profile at 10 K with the analyzing wavelength set on the various components of the transitions to $^7F_1$ and $^7F_2$ (Figure S3 in the Supporting Information) reveals that the compound contains a minor species, II, with $\tilde{\nu}$(0–0) = 17242 cm^{-1} (fwhh = 22 cm^{-1}). Selectively excited emission spectra of I and II are very similar, except for splitting of the $^5D_0 \rightarrow {}^7F_1$ transition, and the lifetimes are alike (1.05 ± 0.01 ms for II at 10 K, as compared with 0.98 ± 0.01 ms for I). Population analysis of the $^5D_0 \rightarrow {}^7F_1$ transition carried out by comparing the emission spectra of the selectively excited species with the broad-band excited spectrum[34] reveals that the minor species accounts for only 3% of the total Eu^{III} population. Several hypotheses are possible, such as the presence of an eight-coordinate species devoid of carboxylate coordination or of an isomer with a different macrocycle conformation; coordination of water is again excluded in view of the long Eu($^5D_0$) lifetime recorded for II.

Analysis of the ligand-field splitting of species I (Table 2) confirms C_4-derived site symmetry for the metal ion. The 0–0 transition has sizeable intensity, as is usually the case for C_n or C_{nv} symmetry. The $^7F_1$ level is split into two components (102 cm^{-1}, allowed magnetic dipole transitions to A and E in the C_4 symmetry point group[34]), while the $^7F_2$ level appears to be unsplit although a weak shoulder can be found on the low-energy side of the corresponding transition (two transitions allowed in C_4 symmetry) which has $I_2/I_1 = 2.40$. Finally, $^5D_0 \rightarrow {}^7F_4$ is comprised of five components, as predicted by the symmetry-related selection rules.

The Tb^{III} spectra are less informative (Figure S4 in the Supporting Information); they feature the usual predominance of the $^5D_4 \rightarrow {}^7F_5$ transition. As for the Eu^{III} complex, the luminescence decays are perfectly single exponential functions and the Tb($^5D_4$) lifetime amounts to 1.30 ± 0.02 ms at 295 K and 1.35 ± 0.02 ms at 10 K. Data recorded at pH values of 3 and 7.5 for TbL^3 confirm the hypothesis of an interaction between the metal ion and the C_5 carboxylic pendant: the hydration number is equal to 2 at acidic pH values, which is consistent with competition between the proton and Tb^{III} for the carboxylate group and, possibly, with partial decomplexation of the macrocyclic ligand. The hydration number drops to $q = 0.64$ at pH 7.5, a value very similar to the one found for TbL^1 ($q = 0.7$ at a pH value close to neutral), a result pointing to an equilibrium between a non-hydrated and a monohydrated species. With respect to the microcrystalline sample, the Eu($^5D_0$) lifetime is shorter in solution and equal to the one reported for EuL^1, for which a hydration number of $q = 0.7$ has been found.[25] Both the Eu($^5D_0$) and Tb($^5D_4$) lifetimes are almost temperature independent between room temperature and 77 K (Table 3), which indicates the absence of temperature-dependent quenching mechanisms.

Table 2. Ligand-field sublevels (major species I, cm^{-1}) identified for microcrystalline EuL^3 from emission spectra at 295 and 10 K. The origin of the energy scale is set on the $^7F_0$ level.

Level	Sublevels at 295 K	Sublevels at 10 K	Level	Sublevels at 295 K	Sublevels at 10 K
$^7F_1$	301	302	$^7F_4$ (cont.)	2855	2864
	403	419		2962	2977
$^7F_2$	1009	1014	$^7F_5$	3940	3956
$^7F_3$	1861	1870		4105	4125
	1936	1942	$^7F_6$	4940	4953
$^7F_4$	2605	2627		5035	5052
	2713	2724		5160	5176
	2787	n.a.[a]	$^5D_0$	17238	17228

[a] n.a.: not applicable.

The quantum yields (Table 3) are smaller than for LnL^1 complexes under the same experimental conditions. The ligand sensitisation efficiency can be estimated for EuL^3 from Equation (10).[35]

$$Q^{Ln}_{L} = \eta_{sens} \times Q^{Ln}_{Ln} = \eta_{sens} \times (\tau_{obs}/\tau_{rad}),$$
$$\text{with } 1/\tau_{rad} = 14.65 \times (I_{tot}/I_{MD}) \times n^3 \ [s^{-1}] \quad (10)$$

In our case, $I_{tot}/I_{MD} = 5.0$ and $n = 1.332$, so $\tau_{rad} = 5.8$ ms, $Q^{Ln}_{Ln} = 10.2\%$ and $\eta_{sens} \approx 19\%$. This figure is relatively low, in line with the observation of substantial triplet emission for this complex; in addition, the intrinsic quantum yield remains small because of water coordination in solution. Quantum yields are pH dependent and this is illustrated in Figure S5 in the Supporting Information for TbL^3, the quantum yield

Table 3. Lifetimes of the Eu($^5D_0$) and Tb($^5D_4$) excited levels, quantum yields and hydration numbers of LnL^3 (Ln: Eu, Tb) in water (or water/glycerol (95:5) for measurements at 77 K) and acetonitrile.

Complex	Solvent	pH value	τ(295 K) [ms]	τ(77 K) [ms]	q_{Ln}[a,b]	q_{Ln}[a,c]	Q^{Ln}_{L} [%][d]
EuL^3	water	6	0.59 ± 0.04	0.67 ± 0.04	–[e]	–[e]	1.9 ± 0.2
	MeCN		0.62 ± 0.04	0.68 ± 0.02	–[e]	–[e]	–[e]
TbL^3	water	3	1.20 ± 0.04	–[e]	2.1	2.0	–[e]
		6	1.66 ± 0.03	1.89 ± 0.04	–[e]	–[e]	3.4 ± 0.3
		7.5	1.97 ± 0.03	–[e]	0.56	0.72	–[e]

[a] From lifetime measurements in water and deuterated water. [b] Estimated according to $q = 5(\Delta k - 0.06)$,[52] with $\Delta k = 1/\tau_{H_2O} - 1/\tau_{D_2O}$. [c] Estimated according to $q = 4.2\ \Delta k$.[53] [d] Absolute quantum yield in aerated water upon ligand excitation; average of measurements with respect to two standards (see the Experimental Section). [e] Not determined.

of which steadily increases for pH 2–6.5 and then sharply decreases for pH values larger than 8 due to the formation of hydroxo species. The drop in the Q_L^{Tb} value between pH 6.5 and 7.5 remains unexplained; it is essentially linked to a weaker emission, with the absorbance remaining relatively constant over this pH range, and may be related to a conformational rearrangement due to acid–base equilibria involving the C_5 pendant as such a behaviour is not observed for TbL^1. In that case, the quantum yield increases from pH 5 to 7 and stays constant up to pH 8.5, before decreasing at more basic pH values.

In view of the interest for LRET experiments,[36] we have investigated the variation in the luminescence intensity and lifetime of 2×10^{-6} M LnL^3 (Ln: Eu, Tb) complexes in water upon addition of Cy5. This fluorescent dye absorbs at 649 nm with a large molar absorption coefficient ($2.5\times10^5\,M^{-1}cm^{-1}$) and emits at 670 nm. Its excited state can, therefore, be populated by transfer from the lanthanide ion. Figure 4 illustrates the transfer from EuL^3 while corresponding data for TbL^3 are shown in Figure S6 in the Supporting Information. As expected from the overlap between the Cy5 absorption spectrum and the Ln emission spectra, transfer is more effective with EuL^3 than with TbL^3.

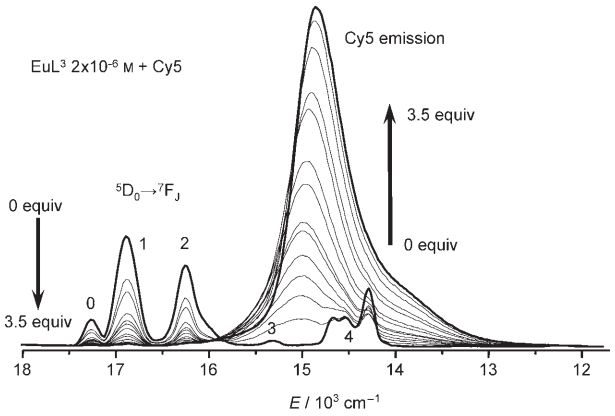

Figure 4. Variation in the emission spectra (uncorrected; excited at 40320 cm^{-1}, 248 nm) of EuL^3 in water at pH 6.5 upon addition of Cy5 (0–3.5 equiv).

The lifetimes of the Ln excited states decrease in parallel with the decrease in metal-centred luminescence, from 0.6 (no Cy5) to 0.06 ms (3.5 equiv of Cy5) for Eu($^5D_0$) and from 1.7 (no Cy5) to 0.16 ms (3 equiv of Cy5) for Tb($^5D_4$). Analysis of the Eu^{III} data in terms of Stern–Volmer plots by using variations in both the Eu^{III} lifetimes and emission intensities is presented in Figure S7 in the Supporting Information. Two concentration domains are evidenced: the first one, approximately up to the addition of 1.5 equivalents Cy5, corresponds to a Stern–Volmer constant of $K^I_{SV}=(3.5\pm0.1)\times10^7\,M^{-1}s^{-1}$ (from emission intensities), while the quenching is more efficient above this ratio, with a doubling in the K^I_{SV} value. On the other hand, the opposite is observed from lifetime data, with the K^τ_{SV} value being smaller by 1.75 in the high-concentration domain. This behaviour probably points to some chemical interaction taking place between Cy5 and the lanthanide complex. The corresponding K^I_{SV} constant for the Tb^{III} system is about 2.5 times smaller, in line with the decreased overlap between the donor-emission and the acceptor-absorption spectra. The collected data allow calculation of the yields of the energy-transfer processes. From Figure 5 (Eu^{III}) and Figure S8 in the Supporting Information (Tb^{III}), one sees that these yields increase sharply up to about one equivalent of added Cy5 and then stabilise. The maximum yield is in the range 90–95 % for EuL^3, while it remains at about 75–80 % for the Tb^{III} chelate.

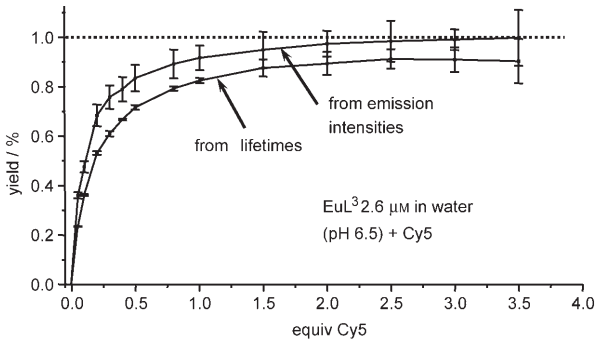

Figure 5. Yield of the EuL^3-to-Cy5 energy transfer at pH 6.5 calculated from both emission-intensity and lifetime data.

Influence of TbL^3 on cell viability: To assess the potential use of the LnL^3 complexes for in vitro analyses, the cytotoxicity of the Tb^{III} complex has been determined with respect to several cell lines, both malignant (5D10 mouse hybridoma, Jurkat human T leukaemia, MCF-7 human breast carcinoma) and non-malignant (HaCat human keratinocyte). In a first step, the influence of the Tb^{III} complex on cell proliferation was determined by using the WST-1 test with measurements after 0.5, 1, 2, 3 and 4 h. As shown at the top of Figure 6 for the MCF-7 and Jurkat cell lines, the absorbance difference ($A_{450}-A_{650}$) increases with time, thereby reflecting the proliferation of the cells. No significant difference can be observed between the proliferation of the cells in the absence or presence of the Tb^{III} complex up to 500 µM for the MCF-7 cell line. The same was true for the HaCat and 5D10 cell lines (Figure S9 in the Supporting Information). On the other hand, a negative influence on cell proliferation can be observed for the Jurkat cell line for concentrations of the complex >125 µM.

These observations were confirmed by the viability of the cells calculated after 24 h of incubation in the presence of various concentrations of TbL^3. Data for the MCF-7 and Jurkat cells are displayed at the bottom of Figure 6. Whereas a negative influence on cell viability was again observed for the Jurkat cell line when the concentration of TbL^3 was larger than 125 µM, no negative effect could be detected for the other three cell lines up to 500 µM. This conclusion is further backed by the lactase dehydrogenase (LDH) assay of cellular membrane damage, the results of which are reported in Table 4. This assay tests the leakage of LDH,

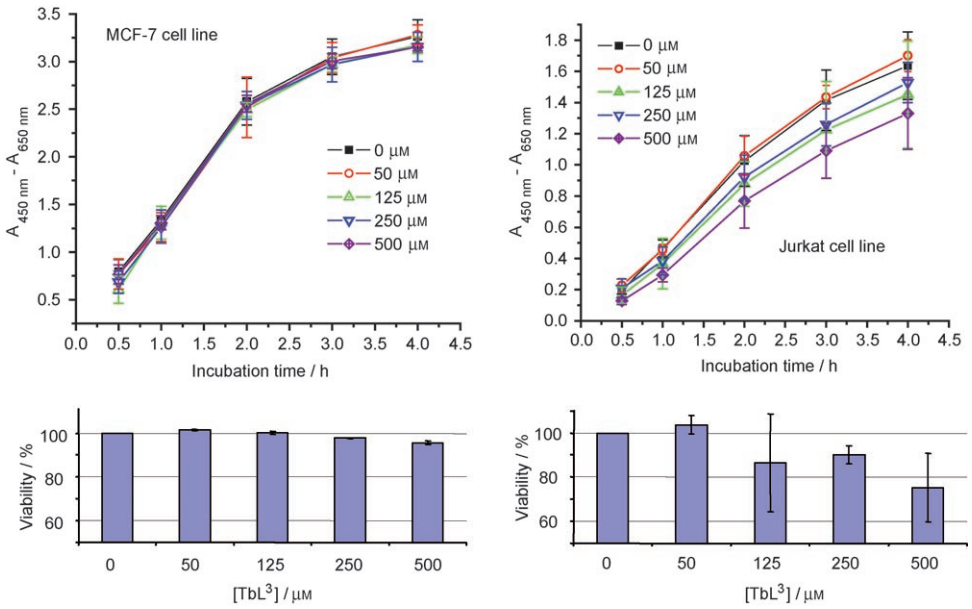

Figure 6. Top: WST-1 proliferation test of cells in the absence or presence of different concentrations of TbL^3. Bottom: Cell viability values (%), obtained by using the same test, for different concentrations of TbL^3 after 24 h incubation at 37 °C.

Table 4. Cell cytotoxicity values [%] measured by using the LDH assay[a] after incubation of the cells with different concentrations of TbL^3.

$[TbL^3]$ [μM]	Jurkat	MCF-7	HaCat
50	0.5 ± 4.6	−5.8 ± 7.5	−11.0 ± 3.9
125	4.0 ± 5.7	−1.9 ± 9.6	−5.9 ± 0.1
250	11.3 ± 5.0	1.1 ± 1.6	−5.5 ± 0.9
500	9.9 ± 3.8	2.6 ± 6.3	−5.6 ± 1.7

[a] At 22 °C and after 30 min of incubation.

which increases if the cell membrane is damaged, that is, if the cell is destroyed. The measured LDH leakage 30 min after incubation with concentrations of TbL^3 ≥250 μM was around 10% for Jurkat cells, while it is close to zero or even slightly negative for the two other cell lines tested, MCF-7 and HaCat. This result means that the latter cell lines do not sustain membrane damage under these experimental conditions.

Conclusion

Modification of L^1 by replacing one chromophoric pendant arm with a C_5 alkyl chain bearing a carboxylic function in L^3 does not influence the stability of the resulting lanthanide chelate LnL^3. On the other hand, the photophysical properties are affected, but the Eu^{III} and Tb^{III} complexes are sufficiently emissive to act as potential luminescent stains. In particular, an efficient LRET phenomenon has been observed and quantified with Cy5. Moreover, interaction of the C_5 pendant with the metal ion is pH dependent and modulates the photophysical properties. The latter, combined with the non-toxicity for several cell lines that has been demonstrated for TbL^3, points to potential in vitro applications of the LnL^3 macrocyclic chelates, which will be tested in future work.

Experimental Section

Materials and methods: Reagents and solvents were purchased from Aldrich, Fluka Ag or Acros; cyclen was from Strem. Solvents were dried by distillation over CaH_2 (CH_2Cl_2, MeCN), Na/benzophenone (THF) or KOH (NEt_3).[37] Lanthanide triflates[38] and perchlorates[39] were prepared in the usual way, from analytical-grade triflic or perchloric acids and high-purity lanthanide oxides (Rhodia). The Ln content was determined by complexometric titration with H_2Na_2(edta) in presence of xylenol orange and urotropine (edta: ethylenediaminetetraacetate).[40]

^{1}H NMR spectra were recorded on a Bruker Avance DRX 400 spectrometer. IR spectra were recorded on a Perkin–Elmer Spectrum One FT spectrometer equipped with an ATR accessory. ESI-MS spectra were measured on a Finningan SSQ-710C instrument. Elemental analyses were performed by Dr H. Eder from the University of Geneva.

Potentiometric titrations: Ligands were titrated in a thermostated (25.0 ± 0.1 °C) glass-jacketed vessel under an Ar atmosphere. The ionic strength was fixed with Me_4NCl (μ = 0.1 M). The solution was acidified to pH ≈ 1.5 with 37% HCl 30 min before titration. Titrations were carried out by using an automatic Metrohm Titrino 736 GP potentiometer (resolution 0.1 mV, accuracy 0.2 mV) linked to an IBM PS/2 computer and by using constant volume addition. An automatic burette (Metrohm 6.3013.210, 10 mL, accuracy 0.03 mL) was used along with a Metrohm 6.0238.000 glass electrode. A standard base solution (NaOH 0.1 M) was added inside the solution through a capillary tip attached to the automatic burette. The data (200 points, drift < 1 mV min^{-1}) were mathematically treated in the program HYPERQUAD2000[41] by using a Marquardt algorithm, and the distribution of species was calculated by using the program HYSS2. Calibration of the pH meter and the electrode system was performed prior to each measurement by using a standardised HCl solution at 25.0 °C: the latter (10 mL) was titrated with a standardised 0.1 M NaOH solution and the electrode potential readings were converted into pH values. The ion product of water (pK_w = 13.91) and the electrode potential were refined by using the program Scientist by Micromath (Version 2.0).

UV/Visible spectra were measured in 1-, 0.2- or 0.1 cm quartz cuvettes on a Perkin–Elmer Lambda 900 spectrometer and the data were analysed with the Specfit software.[42] Speciation of the complexes was determined by batch titration of a 3.3×10^{-5} M ligand solution containing lanthanide perchlorate (Ln: Eu, Tb; 1 equiv). 30–40 samples were prepared with pH values ranging from 1.92–12.24; the ionic strength was kept constant with 0.1 M Me_4NCl. In order to reach thermodynamic equilibrium, samples were kept at 55 °C for one week followed by one day at 25 °C; the pH values and absorption spectra were then measured at this temperature. The data were analysed with the Specfit software.

Luminescence spectra were recorded on a Fluorolog FL-3-22 spectrometer from Spex–Jobin–Yvon–Horiba; quartz cells with optical paths of 1, 0.2 or 0.1 cm were used for room-temperature spectra, while 77 K measurements were carried out on samples put into quartz capillaries with 3 mm diameter. Quantum yields were determined in aerated water with respect to several references: quinine sulphate in 0.5 M sulphuric acid

(QS, $\lambda_{exc}=247$ nm, $Q=54.6\%$[43]) and cresyl violet in methanol (CV, $\lambda_{exc}=258$ nm, $Q=54\%$[44]) for the Tb complex and rhodamine 101 in ethanol (R101, $\lambda_{exc}=255$ nm, $Q=100\%$[45]) and CV for the Eu complex. The absorbance of the samples and references was usually kept under 0.1. The complex concentration was 2×10^{-6} M and Equation (11) was used,[46] in which A is the absorbance, n_D^{20} is the refractive index (1.338, 1.361, 1.328 and 1.332 for QS, R101, CV and the Ln samples, respectively), and S is the integrated, corrected emission area.

$$Q_{abs}^{sample}=\left(\frac{1-10^{-A(ref.)}}{1-10^{-A(sample)}}\right)\times\left(\frac{n_D^{20}(sample)}{n_D^{20}(ref.)}\right)^2\times\frac{S(sample)}{S(ref.)}\times Q_{abs}^{ref.} \qquad (11)$$

N-hydroxysuccinimide-activated Cy5 (abbreviated Cy5) was bought from Amersham and used for the energy-transfer experiments as received.

High-resolution emission spectra and lifetimes were measured on a previously described instrumental setup.[47]

Ligand synthesis (Scheme 2)

*Carboxylic acid substituent **1***: This was synthesised according to the method of Yamada et al.[48] 6-Aminocaproic acid (13.12 g, 0.10 mol) was dissolved in water (100 mL). After being cooled at 0 °C, bromoacetyl bromide (9.55 mL, 0.11 mol) was added dropwise, while the pH value was maintained at 7 with 4 M NaOH (a total of 50 mL was needed). The mixture was stirred for 15 min and the pH value was adjusted to 2 with aqueous HBr (47 %). The resulting solution was concentrated to a volume of 30 mL and extracted with ethyl ether. The combined organic phases were dried over $MgSO_4$, the solvent was evaporated to dryness, diethyl ether (50 mL) was added and the solution was stored at −18 °C for 2 d. The white precipitate was filtered and dried (2.52 g, 0.01 mol, yield = 10 %): m.p. 72 °C; ^{1}H NMR (400 MHz, $CDCl_3$, Me_4Si): $\delta=1.5$–1.8 (m, 6H), 2.3 (t, 2H, $^3J=14.4$ Hz), 3.3 (m, 2H), 3.9 (s, 2H), 6.7 ppm (br, 1H).

*1,4,7,10-Tetraazatricyclo[5.5.1.0]tridecane (**2a**) and 1-formyl-1,4,7,10-tetraazacyclododecane (**2b**)*: Cyclen (5 g, 29 mmol) and *N,N*-dimethylformamide dimethylacetal (3.92 mL, 30.5 mmol) were dissolved in toluene (70 mL) and put into a flask equipped with a Dean–Stark condenser under a nitrogen atmosphere. The methanol/toluene azeotrope formed was distilled until complete elimination of toluene had occurred. The resulting yellow oil (**2a**) was dried overnight at 70 °C. It was then cooled to 0 °C and a water/methanol mixture (1:1 v/v; 25 mL) was added dropwise. The mixture was warmed to room temperature and stirred for 24 h. The solvents were evaporated and the residue was redissolved in a minimum amount of acetonitrile, which was subsequently evaporated; this procedure was repeated twice to completely eliminate water and to yield **2b** as a white solid (5.58 g, 95 % yield): ^{1}H NMR (400 MHz, $CDCl_3$, Me_4Si): $\delta=$ 2.6–2.7 (m, 8H), 3.4 (dt, 8H, $^2J=20.2$, $^3J=5.5$ Hz), 8.0 ppm (s, 1H); IR (ATR): $\tilde{\nu}=3312$ (w, ν_{N-H}), 2811 (m, ν_{C-H}), 1656 (s, $\nu_{C=O}$), 1444 (m, δ_{CH}), 1227 cm^{-1} (m, $\delta_{C=O}$).

*1-Formyl-4,7,10-tris[(*N*-4-phenylacetyl)carbamoylmethyl]-1,4,7,10-tetraazacyclododecane (**4a**)*: Compound **2b** (3.78 g, 189 mmol) was dissolved in THF (100 mL), distilled triethylamine (8.16 mL, 586 mmol) was added and the solution was stirred for 1 h under an inert atmosphere. A solution of **3** (15.0 g, 585 mmol) in anhydrous THF (100 mL) was added and the mixture was stirred at room temperature for 2 d. A white precipitate of triethylbromide was filtered off and the solution was concentrated. The beige product **4a** (9.37 g, 65 % yield) precipitated upon addition of diethyl ether: ^{1}H NMR (400 MHz, $CDCl_3$, Me_4Si): $\delta=2.8$–3.3 (m, 16H), 3.7 (s, 1H), 4.6 (d, 2H, $^3J=4.4$ Hz), 4.7 (d, 2H, $^3J=5$ Hz), 4.7 (d, 2H, $^3J=5.2$ Hz), 7.3–8.0 (m, 15H), 8.1 ppm (s, 1H); ESI-MS: *m/z*: 726 [**4a**+H]$^+$, 748 [**4a**+Na]$^+$.

*1,4,7-Tris[(*N*-4-phenylacetyl)carbamoylmethyl]-1,4,7,10-tetraazacyclododecane (**4b**)*: Compound **4a** (7.41 g, 102 mmol) was dissolved in a mixture of acetone (75 mL) and water (40 mL) and cooled to 0 °C before concentrated HCl (37 %; 45 mL) was added dropwise. The resulting solution became orange and was stirred for 4 d at room temperature. A saturated solution of $NaHCO_3$ was added until the pH value reached 7 (≈500 mL) and the compound was extracted with CH_2Cl_2 (3×400 mL). The combined organic phases were dried over $MgSO_4$ and filtered, then the solvent was evaporated. An orange oil was collected which solidified after drying under vacuum: ^{1}H NMR (400 MHz, $CDCl_3$, Me_4Si): $\delta=2.8$ (s, 10H), 2.9 (s, 6H), 3.3 (s, 4H), 3.3 (s, 2H), 4.5 (d, 4H, $^3J=5.4$ Hz), 4.6 (d, 2H, $^3J=5.5$ Hz), 7.4–7.9 (m, 15H), 8.0 ppm (s, 1H); IR (ATR): $\tilde{\nu}=3290$ (w, br, ν_{N-H}), 3060 (w, $\nu_{C-H(ar)}$), 2924, 2831 (w, ν_{CH}), 1695 (s, $\nu_{C=O(phen)}$), 1652 (s, $\nu_{C=O(am)}$), 1596 (m, $\nu_{C=C}$), 1579 (w, $\nu_{C=C}$), 1525 (s, $\nu_{C=C}$, $\nu_{C=O(am)}$), 1448 (s, δ_{C-H}), 1221 (s, δ_{C-O}), 755 (s, $\delta_{C-H(ar)}$), 688 cm^{-1} (s, $\delta_{C-H(ar)}$); ESI-MS: *m/z*: 698 [**4b**+H]$^+$, 349 [**4b**+2H]$^{2+}$.

*1,4,7-Tris[(*N*-4-phenylacetyl)carbamoylmethyl]-10-[*N*-(carboxypentyl)carbamoylmethyl]-1,4,7,10-tetraazacyclododecane (L^3)*: Compound **4b** (1.383 g, 2 mmol) was dissolved with $CsCO_3$ (0.646 g, 2 mmol) in anhydrous acetonitrile (200 mL) and the mixture was stirred under a controlled atmosphere for 30 min. A solution of **1** (0.474 g, 2 mmol) in anhydrous acetonitrile (100 mL) was added and the mixture was stirred at room temperature for 3 d. A white precipitate was filtered from the resulting yellow solution and the solvent was evaporated to leave a yellow solid which was purified on a cationic Dowex 50W X 8 resin followed by an anionic chloride resin (Amberlite): Yield = 0.516 g (30 %); ^{1}H NMR (400 MHz, $CDCl_3$, Me_4Si): $\delta=1.1$ (m, 2H), 1.2 (m, 2H), 1.4 (m, 2H), 2.1 (t, 2H, $^3J=5.5$ Hz), 2.8–3.0 (m, 18H), 3.4 (s, 2H), 3.5 (s, 4H), 3.5 (s, 2H), 4.4 (d, 2H, $^3J=5.5$ Hz), 4.5 (d, 4H, $^3J=5.3$ Hz), 7.4–7.8 ppm (m, 15H); ^{13}C NMR (800 MHz, MeOD) $\delta=196.16$ (Ph−C=O), 173.78 (CO_2H), 172.59 (NH−C=O), 136.70, 136.65 (C_{ar}), 135.51, 135.44, 135.63 (CH_{ar}), 133.70 (CH_{ar}), 131.08 (CH_{ar}), 130.48, 130.43, 130.25 (CH_{ar}), 129.74, 129.58, 129.49 (CH_{ar}), 63.09 ($COCH_2N$), 58.83, 58.74 ($COCH_2N$), 58.74 ($COCH_2$), 50.00, 49.83, 49.78 and 49.69 (CH_2-CH_2), 47.85 ($COCH_2NH$), 40.72, 40.23 (CH_2), 36.46, 35.85 (CH_2), 30.76, 30.48 (CH_2), 28.05, 28.01 (CH_2), 26.52, 26.44 ppm (CH_2); IR (ATR): $\tilde{\nu}=3300$ (w, br, ν_{O-H}, ν_{N-H}), 3062 (w, $\nu_{C-H(ar)}$), 2933, 2854, 2831 (w, ν_{C-H}), 1694 (m, $\nu_{C=O(Phen)}$), 1657 (s, $\nu_{C=O(ac)}$), 1652 (s, $\nu_{C=O(am)}$), 1596 (m, $\nu_{C=C(ar)}$), 1579 (w, $\nu_{C=C(ar)}$), 1544 (sh, $\nu_{C=O(ac)}$), 1530 (s, $\nu_{C=C(ar)}$, $\nu_{C=O(am)}$), 1448 (m, δ_{C-H}), 1222 (s, δ_{C-O}), 755, 688 cm^{-1} (s, $\delta_{C-H(ar)}$); ESI-MS: *m/z*: 869 [L^3+H]$^+$, 435 [L^3+2H]$^{2+}$; elemental analysis: calcd (%) for $L^3{\cdot}2H_2O{\cdot}HCl$ ($C_{46}H_{65}ClN_8O_{11}$): C 58.68, H 6.96, N 11.90; found: C 58.73, H 7.01, N 12.06.

*1,4,7-Tris[(*N*-4-phenylacetyl)carbamoylmethyl]-10-[*N*-(methanopentyl)carbamoylmethyl]-1,4,7,10-tetraazacyclododecane (L^4)*: Ligand L^3 (0.1 g, 0.11 mmol) was dissolved in anhydrous ethanol (40 mL) and the solution was refluxed overnight. The solvent was evaporated and the product was recrystallised in hot acetonitrile (0.042 g, 43 % yield): ^{1}H NMR (400 MHz, $CDCl_3$, Me_4Si): $\delta=1.1$ (m, 2H), 1.2 (m, 2H), 1.3 (m, 2H), 2.1 (t, 2H, $^3J=5.5$ Hz), 2.8–3.0 (m, 18H), 3.4 (s, 2H), 3.5 (s, 4H), 3.5 (s, 2H), 3.67 (s, 3H), 4.4 (d, 2H, $^3J=5.5$ Hz), 4.5 (d, 4H, $^3J=5.3$ Hz), 7.4–7.8 ppm (m, 15H); ESI-MS: *m/z*: 884 [L^4+H]$^+$, 443 [L^4+2H]$^{2+}$; elemental analysis: calcd (%) for $L^4{\cdot}H_2O{\cdot}HCl$ ($C_{47}H_{65}ClN_8O_{10}$): C 60.21, H 6.99, N 11.95; found: C 60.40, H 7.03, N 11.99.

Synthesis of the complexes: $Ln(OTf)_3{\cdot}x\,H_2O$ ($x=0$–2; 1 equiv) was mixed with ligand (1 equiv) in acetonitrile. The solution was refluxed for 3 d and the $[Ln(OTf)_3L^3]{\cdot}n\,MeCN{\cdot}m\,H_2O$ complexes were then precipitated by addition of CH_2Cl_2 and dried under vacuum. Elemental analyses of the products are reported in Table 5.

Cell culture: Cell viability was tested on the following cell lines: mouse hybridoma 5D10, human T leukaemia Jurkat (ATCC TIB152), human breast adenocarcinoma MCF-7 (ATCC HTB-22) and non-malignant epithelial HaCat (human keratinocytes). Cells were cultivated in 75 cm^2 cul-

Table 5. Elemental analyses for the isolated $[Ln(OTf)_3(L^3)]{\cdot}n\,MeCN{\cdot}m\,H_2O$ complexes. Calculated values are in parentheses.

Ln	*n*	*m*	Formula	C [%]	H [%]	N [%]
Eu	0	6	$C_{51}H_{75}F_9N_9O_{24}S_3Eu$	37.52 (37.34)	4.79 (4.60)	6.95 (7.11)
Tb	0.5	6.5	$C_{100}H_{149}F_{18}N_{17}O_{49}S_6Tb_2$	36.99 (37.24)	4.40 (4.66)	7.55 (7.38)
Gd	0	6	$C_{49}H_{72}F_9N_8O_{24}S_3Gd$	37.33 (37.21)	4.75 (4.59)	6.96 (7.08)
Lu	0	7	$C_{49}H_{74}F_9N_8O_{25}S_3Lu$	36.45 (36.39)	4.76 (4.61)	6.54 (6.93)

ture flasks by using RPMI 1640 medium supplemented with 10% foetal calf serum (FCS), 2 mM L-glutamine, 1 mM sodium pyruvate, 1% non-essential amino acids and 1% sodium [4-(2-hydroxyethyl)piperazine-1-ethanesulfonate monosodium salt (HEPES; all from Gibco Cell Culture, Invitrogen, Basel, Switzerland). Cultures were maintained at 37°C under a 5% CO_2 and 95% air atmosphere. The growth medium was changed every other day until the time of use of the cells. The cell density and viability, defined as the ratio of the number of viable cells over the total number of cells, of the cultures were determined by trypan blue staining and use of a Neubauer improved hemacytometer (Blau Brand, Wertheim, Germany). Prior to each viability test, the cells were harvested and diluted at a density of 7.5×10^5 cells mL^{-1}. The cell suspension was seeded into 96-well plates at a concentration of 100 μL per well and incubated overnight at 37°C and under 5% CO_2 prior to addition of the TbL^3 complex and the WST-1 or LDH reagent.

WST-1 cell viability test: Cell-proliferation reagent WST-1 (Roche, Germany) is a slightly red tetrazolium salt that is reduced only in living metabolically active cell mitochondria to yield a dark-red formazan dye which can be quantified spectrophotometrically.[49] Cells were seeded in a 96-well tissue-culture microplate at a concentration of 7.5×10^4 cells per well in culture medium (100 μL) and then incubated overnight at 37°C and under 5% CO_2. The TbL^3 complex was dissolved in fresh RPMI medium at 37°C and at a concentration of 500 μM. The medium was removed from the cell cultures and the TbL^3 chelate was added (100 μL per well; final concentrations: 500, 250, 125 and 50 μM). WST-1 reagent (10 μL) was added to each well and the plate was shaken for 1 min on a microtiter-plate shaker (450 rpm). The plate was further incubated at 37°C and under 5% CO_2 and the absorbance of the formazan product was measured at 450 nm with an ELISA reader (Spectra MAX 340, Molecular Devices, Sunnyvale, CA, USA). The cell viability was calculated from the absorbance values according to Equation (12), in which $(A_{450}-A_{650})$ is the difference between the absorbances at 450 and 650 nm for the cells put into contact with TbL^3 (exp) or with the medium only (medium). Results are expressed as averages over four nominally identical measurements.

$$viability_{WST}\ [\%] = \frac{(A_{450}-A_{650})_{exp}}{(A_{450}-A_{650})_{medium}} \times 100 \qquad (12)$$

LDH cell toxicity test: Lactate dehydrogenase (LDH) leakage was measured by using the CytoTox 96 non-radioactive cytotoxicity assay kit (Promega Corporation, Madison, WI, USA).[50,51] Cells were seeded in a 96-well tissue-culture microplate at a concentration of 7.5×10^4 cells per well in culture medium (100 μL) and then incubated overnight at 37°C and under 5% CO_2. The TbL^3 complex was dissolved in fresh RPMI medium at 37°C and at a concentration of 500 μM. The medium was removed from the cell cultures and the TbL^3 complex was added (100 μL per well; final concentrations: 500, 250, 125 and 50 μM). The substrate mixture solution (50 μL) was then added. The plates were incubated at 22°C for 30 min. The LDH released from the cells catalyses the conversion of resazurin into resorufin. After incubation of the mixture, the fluorescence values were measured with an excitation wavelength of 530 nm and an emission wavelength of 590 nm in a microplate fluorometer (Cytofluor series 4000, Perceptive Biosystems, Framingham, MA, USA). The results are expressed as averages of four nominally identical measurements. The maximum LDH release after cell lysis with Triton X-100 (9 vol%) and the spontaneously released LDH in cells not in contact with the TbL^3 complex were also measured. The average fluorescence values of the culture-medium background were subtracted from all fluorescence values of experimental wells. Cytotoxicity caused by the TbL^3 complex was calculated according to Equation (13).

$$cytotoxicity_{LDH}\ [\%] = \frac{I_{exp}-I_{medium}}{I_{exp,max}-I_{medium}} \times 100 \qquad (13)$$

I_{exp} is the fluorescence value of the cells in contact with different concentrations of the TbL^3 complex, I_{medium} is the fluorescence value for the spontaneous release of LDH by cells not in contact with the TbL^3 complex and $I_{exp,max}$ is the fluorescence value for lysed cells with maximum LDH release.

Acknowledgements

This research is supported by the Swiss National Science Foundation. We are indebted to Dr. T. Peymann for preliminary work on the ligand synthesis and to Dr. Anjum Dadabhoy for valuable advice. We thank Prof. F. Wurm (École Polytechnique Fédérale de Lausanne, Switzerland) for the use of his Spectra MAX340 ELISA reader and Cytofluor series 4000 fluorimeter. The 5D10 hybridoma cell line was a gift from the Biomedical Research Institute "Dr. L. Willems Instituut" (University of Hasselt, Belgium).

[1] H. Stetter, W. Frank, *Angew. Chem.* **1976**, *88*, 760; *Angew. Chem. Int. Ed. Engl.* **1976**, *15*, 786.
[2] J. F. Desreux, *Bull. Acad. R. Belg.* **1979**, *64*, 814–814.
[3] C. A. Chang, L. C. Francesconi, M. F. Malley, K. Kumar, J. Z. Gougoutas, M. F. Tweedle, D. W. Lee, L. J. Wilson, *Inorg. Chem.* **1993**, *32*, 3501–3508.
[4] A. Bianchi, L. Calabi, F. Corana, S. Fontana, P. Losi, A. Maiocchi, L. Paleari, B. Valtancoli, *Coord. Chem. Rev.* **2000**, *204*, 309–393.
[5] J. F. Desreux, P. P. Barthelemy, *Nucl. Med. Biol.* **1988**, *15*, 9–15.
[6] P. Caravan, *Chem. Soc. Rev.* **2006**, *35*, 512–523.
[7] J.-C. G. Bünzli, C. Piguet, *Chem. Soc. Rev.* **2005**, *34*, 1048–1077.
[8] I. Hemmilä, V. M. Mukkala, *Crit. Rev. Clin. Lab. Sci.* **2001**, *38*, 441–519.
[9] S. Faulkner, J. L. Matthews in *Comprehensive Coordination Chemistry II, Vol. 9* (Ed.: M. D. Ward), Elsevier Pergamon, Amsterdam, **2004**, pp. 913–944.
[10] M. Li, P. R. Selvin, *J. Am. Chem. Soc.* **1995**, *117*, 8132–8138.
[11] D. Parker, J. A. G. Williams, *J. Chem. Soc. Perkin Trans. 2* **1996**, 1581–1586.
[12] A. Beeby, D. Parker, J. A. G. Williams, *J. Chem. Soc. Perkin Trans. 2* **1996**, 1565–1579.
[13] D. Parker, *Chem. Soc. Rev.* **2004**, *33*, 156–165.
[14] D. Parker, J. A. G. Williams in *Responsive luminescent lanthanide complexes* (Eds.: A. Sigel, H. Sigel), Metal Ions in Biological Systems, *Vol. 40*, Marcel Dekker, New York, **2003**.
[15] D. Parker, R. S. Dickins, H. Puschmann, C. Crossland, J. A. K. Howard, *Chem. Rev.* **2002**, *102*, 1977–2010.
[16] D. Parker, *Coord. Chem. Rev.* **2000**, *205*, 109–130.
[17] L. Armelao, G. Bottaro, S. Quici, M. Cavazzani, M. C. Raffo, F. Barigelletti, G. Accorsi, *Chem. Commun.*, **2007**, 1911–2913.
[18] S. Faulkner, S. J. A. Pope, B. P. Burton-Pye, *Appl. Spectrosc. Rev.* **2005**, *40*, 1–31.
[19] S. Pandya, J. H. Yu, D. Parker, *Dalton Trans.* **2006**, 2757–2766.
[20] J.-C. G. Bünzli, *Acc. Chem. Res.* **2006**, *39*, 53–61.
[21] "Lanthanide Near-Infrared Luminescence in Molecular Probes and Devices": S. Comby, J.-C. G. Bünzli in *Handbook on the Physics and Chemistry of Rare Earths, Vol. 37* (Eds.: K. Gschneidner, Jr., J.-C. G. Bünzli, V. Pecharsky), Elsevier Science, Amsterdam, **2007**, Chapter 235.
[22] G. Zucchi, R. Scopelliti, P. A. Pittet, J.-C. G. Bünzli, R. D. Rogers, *J. Chem. Soc. Dalton Trans.* **1999**, 931–938.
[23] G. Zucchi, R. Scopelliti, J.-C. G. Bünzli, *J. Chem. Soc. Dalton Trans.* **2001**, 1975–1985.
[24] K. N. Raymond, G. Müller, F. Matzanke, *Top. Curr. Chem.* **1984**, *123*, 49–102.
[25] G. Zucchi, A.-C. Ferrand, R. Scopelliti, J.-C. G. Bünzli, *Inorg. Chem.* **2002**, *41*, 2459–2465.
[26] I. Hemmilä, T. Ståhlberg, P. Mottram, *Bioanalytical Applications of Labelling Technologies*, Wallac Oy, Turku, **1995**.
[27] P. R. Selvin, *Annu. Rev. Biophys. Biomol. Struct.* **2002**, *31*, 275–302.
[28] H. Bazin, E. Trinquet, G. Mathis, *Rev. Mol. Biotechnol.* **2002**, *82*, 233–250.
[29] C. Glogard, R. Hovland, S. L. Fossheim, A. J. Aasen, J. Klaveness, *J. Chem. Soc. Perkin Trans. 2* **2000**, 1047–1052.
[30] J. H. Yu, D. Parker, *Eur. J. Org. Chem.* **2005**, 4249–4252.
[31] J. Platzek, P. Blaszkiewicz, H. Gries, P. Luger, G. Michl, A. Muller-Fahrnow, B. Raduchel, D. Sulzle, *Inorg. Chem.* **1997**, *36*, 6086–6093.

[32] A. Bianchi, L. Calabi, C. Giorgi, P. Losi, P. Mariani, Paoli, P. Rossi, B. Valtancoli, M. Virtuani, *J. Chem. Soc. Dalton Trans.* **2000**, 697–705.
[33] S. T. Frey, W. deW. Horrocks, Jr., *Inorg. Chim. Acta* **1995**, *229*, 383–390.
[34] J.-C. G. Bünzli in *Lanthanide Probes in Life, Chemical and Earth Sciences: Theory and Practice* (Eds.: J.-C. G. Bünzli, G. R. Choppin), Elsevier Science, Amsterdam, **1989**, pp. 219–293.
[35] M. H. V. Werts, R. T. F. Jukes, J. W. Verhoeven, *Phys. Chem. Chem. Phys.* **2002**, *4*, 1542–1548.
[36] "Lanthanide Chelates as Luminescent Labels in Biomedical Analyses": K. Nishioka, K. Fukui, K. Matsumoto in *Handbook on the Physics and Chemistry of Rare Earths, Vol. 37* (Eds.: K. Gschneidner, Jr., J.-C. G. Bünzli, V. Pecharsky), Elsevier Science, Amsterdam, **2007**, Chapter 234.
[37] D. D. Perrin, W. L. F. Armarego, *Purification of Laboratory Chemicals*, Pergamon Press, Oxford, **1988**.
[38] J.-C. G. Bünzli, F. Pilloud, *Inorg. Chem.* **1989**, *28*, 2638–2642.
[39] J.-C. G. Bünzli, C. Mabillard, *Inorg. Chem.* **1986**, *25*, 2750–2754.
[40] G. Schwarzenbach, *Complexometric Titrations*, Chapman & Hall, London, **1957**.
[41] L. Alderighi, P. Gans, A. Ienco, D. C. Peters, A. Sabatini, A. Vacca, *Coord. Chem. Rev.* **1999**, 311–318.
[42] H. Gampp, M. Maeder, C. J. Meyer, A. D. Zuberbühler, *Talanta* **1986**, *33*, 943–951.
[43] S. R. Meech, D. C. Phillips, *J. Photochem.* **1983**, *23*, 193–217.
[44] D. F. Eaton, *Pure Appl. Chem.* **1988**, *60*, 1107–1114.
[45] T. Karstens, K. Kobs, *J. Phys. Chem.* **1980**, *84*, 1871–1872.
[46] B. Fanget, O. Devos, M. Draye, *Anal. Chem.* **2003**, *75*, 2790–2795.
[47] R. Rodriguez-Cortinas, F. Avecilla, C. Platas-Iglesias, D. Imbert, J.-C. G. Bünzli, A. de Blas, T. Rodriguez-Blas, *Inorg. Chem.* **2002**, *41*, 5336–5349.
[48] H. Yamada, F. Uozumi, A. Ishikawa, T. Imoto, *J. Biochem.* **1984**, *95*, 503–510.
[49] M. Ishiyama, K. Sasamoto, M. Shiga, Y. Ohkura, K. Ueno, K. Nishiyama, I. Taniguchi, *Analyst* **1995**, *120*, 113–116.
[50] C. Korzeniewski, D. M. Callewaert, *J. Immunol. Methods* **1983**, *64*, 313–320.
[51] T. Decker, M. L. Lohmannmatthes, *J. Immunol. Methods* **1988**, *115*, 61–69.
[52] A. Beeby, I. M. Clarkson, R. S. Dickins, S. Faulkner, D. Parker, L. Royle, A. S. de Sousa, J. A. G. Williams, M. Woods, *J. Chem. Soc. Perkin Trans. 2* **1999**, 493–503.
[53] W. deW. Horrocks, Jr., D. R. Sudnick, *J. Am. Chem. Soc.* **1979**, *101*, 334–335.

Received: May 30, 2007
Published online: September 14, 2007

